

# Two octaves mid-infrared supercontinuum generation in As<sub>2</sub>Se<sub>3</sub> microwires

Alaa Al-kadry,<sup>1,\*</sup> Mohammed El Amraoui,<sup>2</sup> Younès Messaddeq,<sup>2</sup> and  
Martin Rochette<sup>1</sup>

<sup>1</sup>*Department of Electrical and Computer Engineering, McGill University, Montréal, QC, H3A  
2A7, Canada*

<sup>2</sup>*Center for Optics, Photonics and Lasers (COPL), Laval University, Québec City, QC, G1V  
0A6, Canada*

[\\*alaa.al-kadry@mail.mcgill.ca](mailto:alaa.al-kadry@mail.mcgill.ca)

**Abstract:** We report the first demonstration of mid-infrared supercontinuum generation in As<sub>2</sub>Se<sub>3</sub> chalcogenide microwires with the added advantage of using low energy pulses. The generated SC covers two octaves of bandwidth from 1.1  $\mu\text{m}$  to 4.4  $\mu\text{m}$  at -30 dB. This exceeds the broadest reported SC bandwidth in As<sub>2</sub>Se<sub>3</sub> microwires by a factor of 3.5. The microwire geometry and pumping conditions are the key parameters in generating the 3.3  $\mu\text{m}$  bandwidth while using a low pump pulse energy of 500 pJ.

© 2014 Optical Society of America

**OCIS codes:** (190.0190) Nonlinear optics; (320.0320) Ultrafast optics; (060.5530) Pulse propagation and solitons; (060.4370) Nonlinear optics, fibers; (230.6080) Sources.

---

## References and links

1. I. Hartl, X. D. Li, C. Chudoba, R. K. Ghanta, T. H. Ko, J. G. Fujimoto, J. K. Ranka, and R. S. Windeler, "Ultrahigh-resolution optical coherence tomography using continuum generation in an air-silica microstructure optical fiber," *Opt. Lett.* **26**, 608–610 (2001).
2. A. Labruyère, A. Tonello, V. Couderc, G. Huss, and P. Leproux, "Compact supercontinuum sources and their biomedical applications," *Opt. Fiber Technol.* **18**, 375–378 (2012).
3. S. Sanders, "Wavelength-agile fiber laser using group-velocity dispersion of pulsed super-continua and application to broadband absorption spectroscopy," *Appl. Phys. B* **75**, 799–802 (2002).
4. R. R. Gattass, L. B. Shaw, V. Q. Nguyen, P. C. Pureza, I. D. Aggarwal, and J. S. Sanghera, "All-fiber chalcogenide-based mid-infrared supercontinuum source," *Opt. Fiber Technol.* **18**, 345–348 (2012).
5. L. B. Shaw, P. A. Thielen, F. H. Kung, V. Q. Nguyen, J. S. Sanghera, and I. D. Aggarwal, "IR supercontinuum generation in As-Se photonic crystal fiber," *Conf. Adv. Solid State Lasers (ASSL)*, (2005).
6. J. Hu, C. R. Menyuk, L. B. Shaw, J. S. Sanghera, and I. D. Aggarwal, "Maximizing the bandwidth of supercontinuum generation in as<sub>2</sub>se<sub>3</sub> chalcogenide fibers," *Opt. Express* **18**, 6722–6739 (2010).
7. R. R. Gattass, L. B. Shaw, and J. S. Sanghera, "Microchip laser mid-IR Supercontinuum laser source based on As<sub>2</sub>Se<sub>3</sub> fiber," *Opt. Lett.* **39**, 3418–3420 (2014).
8. L. B. Shaw, R. R. Gattass, J. Sanghera, and I. Aggarwal, "All-fiber mid-IR supercontinuum source from 1.5 to 5  $\mu\text{m}$ ," *Proc. SPIE7914*, 79140P (2011).
9. J. Price, T. M. Monro, H. Ebendorff-Heidepriem, F. Poletti, P. Horak, V. Finazzi, J. Leong, P. Petropoulos, J. C. Flanagan, G. Brambilla, X. Feng, and D. J. Richardson, "Mid-IR supercontinuum generation from nonsilica microstructured optical fibers," *IEEE J. Sel. Top. Quant.* **13**, 738–749 (2007).
10. N. Ducros, A. Labruyère, S. Février, F. Morin, F. Druon, M. Hanna, P. Georges, R. Buczynski, D. Pysz, and R. Stepien, "Mid-infrared supercontinuum generation in lead-bismuth-gallium oxide glass photonic crystal fiber," in *Conference on Lasers and Electro-Optics*, (Optical Society of America, 2010).
11. A. M. Heidt, J. H. V. Price, C. Baskiotis, J. S. Feehan, Z. Li, S. U. Alam, and D. J. Richardson, "Mid-infrared ZBLAN fiber supercontinuum source using picosecond diode-pumping at 2  $\mu\text{m}$ ," *Opt. Express* **21**, 24281–24287 (2013).

12. O. P. Kulkarni, V. V. Alexander, M. Kumar, M. J. Freeman, M. N. Islam, F. L. Terry Jr, M. Neelakandan, A. Chan, "Supercontinuum generation from 1.9 to 4.5  $\mu\text{m}$  in zblan fiber with high average power generation beyond 3.8  $\mu\text{m}$  using a thulium-doped fiber amplifier," *J. Opt. Soc. Am. B* **28**, 2486–2498 (2011).
13. P. Domachuk, N. A. Wolchover, M. Cronin-Golomb, A. Wang, A. K. George, C. M. B. Cordeiro, J. C. Knight, and F. G. Omenetto, "Over 4000 nm bandwidth of mid-IR supercontinuum generation in sub-centimeter segments of highly nonlinear tellurite PCFs," *Opt. Express* **16**, 7161–7168 (2008).
14. I. Savelli, O. Mouawad, J. Fatome, B. Kibler, F. Désévéday, G. Gadret, J.-C. Jules, P. Bony, H. Kawashima, W. Gao, T. Kohoutek, T. Suzuki, Y. Ohishi, and F. Smektala, "Mid-infrared 2000-nm bandwidth supercontinuum generation in suspended-core microstructured sulfide and tellurite optical fibers," *Opt. Express* **20**, 27083–27093 (2012).
15. I. D. Aggarwal and J. S. Sanghera, "Development and applications of chalcogenide glass optical fibers at NRL," *J. Optoelectron. Adv. Mater* **4**, 665–678 (2002).
16. J. M. Harbold, F. O. Ilday, F. W. Wise, J. S. Sanghera, V. Q. Nguyen, L. B. Shaw, and I. D. Aggarwal, "Highly nonlinear as-s-se glasses for all-optical switching," *Opt. Lett.* **27**, 119–121 (2002).
17. D.-H. Yeom, E. C. Mgi, M. R. E. Lamont, M. A. F. Roelens, L. Fu, and B. J. Eggleton, "Low-threshold supercontinuum generation in highly nonlinear chalcogenide nanowires," *Opt. Lett.* **33**, 660–662 (2008).
18. T. M. Monro, Y. D. West, D. W. Hewak, N. G. R. Broderick, and D. J. Richardson, "Chalcogenide holey fibres," *Electron. Lett.* **36**, 1998–2000 (2000).
19. M. Duhant, W. Renard, G. Canat, J. Trols, P. Toupin, L. Brilland, F. Smektala, A. Btourn, P. Bourdon, and G. Renversez, "Mid-infrared strong spectral broadening in microstructured tapered chalcogenide AsSe fiber," *Proc. SPIE8237*, 823735 (2012).
20. E. C. Mägi, L. B. Fu, H. C. Nguyen, M. R. Lamont, D. I. Yeom, and B. J. Eggleton, "Enhanced kerr nonlinearity in sub-wavelength diameter as<sub>2</sub>se<sub>3</sub> chalcogenide fiber tapers," *Opt. Express* **15**, 10324–10329 (2007).
21. M. El-Amraoui, G. Gadret, J. C. Jules, J. Fatome, C. Fortier, F. Dsvdavy, I. Skripatchev, Y. Messaddeq, J. Troles, L. Brilland, W. Gao, T. Suzuki, Y. Ohishi, and F. Smektala, "Microstructured chalcogenide optical fibers from As<sub>2</sub>S<sub>3</sub> glass: towards new IR broadband sources," *Opt. Express* **18**, 26655–26665 (2010).
22. J. S. Sanghera, S. B. Shaw, and I. D. Aggarwal, "Chalcogenide glass-fiber-based mid-IR sources and applications," *IEEE J. Sel. Top. Quant.* **15**, 114–119 (2009).
23. W. Gao, M. El Amraoui, M. Liao, H. Kawashima, Z. Duan, D. Deng, T. Cheng, T. Suzuki, Y. Messaddeq, and Y. Ohishi, "Mid-infrared supercontinuum generation in a suspended-core As<sub>2</sub>S<sub>3</sub> chalcogenide microstructured optical fiber," *Opt. Express* **21**, 9573–9583 (2013).
24. O. Mouawad, J. Picot-Clmente, F. Amrani, C. Strutynski, J. Fatome, B. Kibler, F. Dsvdavy, G. Gadret, J.-C. Jules, D. Deng, Y. Ohishi, and F. Smektala, "Multioctave midinfrared supercontinuum generation in suspended-core chalcogenide fibers," *Opt. Lett.* **39**, 2684–2687 (2014).
25. A. Marandi, C. W. Rudy, V. G. Plotnichenko, E. M. Dianov, K. L. Vodopyanov, and R. L. Byer, "Mid-infrared supercontinuum generation in tapered chalcogenide fiber for producing octave-spanning frequency comb around 3  $\mu\text{m}$ ," *Opt. Express* **20**, 24218–24225 (2012).
26. C. W. Rudy, A. Marandi, K. L. Vodopyanov, and R. L. Byer, "Octave-spanning supercontinuum generation in in situ tapered As<sub>2</sub>S<sub>3</sub> fiber pumped by a thulium-doped fiber laser," *Opt. Lett.* **38**, 2865–2868 (2013).
27. S. Shabahang, M. P. Marquez, G. Tao, M. U. Piracha, D. Nguyen, P. J. Delfyett, and A. F. Abouraddy, "Octave-spanning infrared supercontinuum generation in robust chalcogenide nanotapers using picosecond pulses," *Opt. Lett.* **37**, 4639–4641 (2012).
28. B. J. Eggleton, B. Luther-Davies, and K. Richardson, "Chalcogenide photonics," *Nat. Photonics* **5**, 141–148 (2011).
29. C. Wei, X. Zhu, R. A. Norwood, F. Song, and N. Peyghambarian, "Numerical investigation on high power mid-infrared supercontinuum fiber lasers pumped at 3 $\mu\text{m}$ ," *Opt. Express* **21**, 29488–29504 (2013).
30. I. Kubat, C. S. Agger, U. Møller, A. B. Seddon, Z. Tang, S. Sujecki, T. M. Benson, D. Furniss, S. Lamrini, K. Scholle, P. Fuhrberg, B. Napier, M. Farries, J. Ward, P. M. Moselund, and O. Bang, "Mid-infrared supercontinuum generation to 12.5  $\mu\text{m}$  in large NA chalcogenide step-index fibres pumped at 4.5  $\mu\text{m}$ ," *Opt. Express* **22**, 19169–19182 (2014).
31. A. Al-kadry and M. Rochette, "Broadband supercontinuum generation in As<sub>2</sub>Se<sub>3</sub> chalcogenide wires by avoiding the two-photon absorption effects," *Opt. Lett.* **38**, 1185–1187 (2013).
32. D. D. Hudson, S. A. Dekker, E. C. Mgi, A. C. Judge, S. D. Jackson, E. Li, J. S. Sanghera, L. B. Shaw, I. D. Aggarwal, and B. J. Eggleton, "Octave spanning supercontinuum in an As<sub>2</sub>S<sub>3</sub> taper using ultralow pump pulse energy," *Opt. Lett.* **36**, 1122–1124 (2011).
33. C. Baker and M. Rochette, "A generalized heat-brush approach for precise control of the waist profile in fiber tapers," *Opt. Mater. Express* **1**, 1065–1076 (2011).
34. G. Zhai and L. Tong, "Roughness-induced radiation losses in optical micro or nanofibers," *Opt. Express* **15**, 13805–13816 (2007).
35. J. Teipel, K. Franke, D. Törke, F. Warken, D. Meiser, M. Leuschner, and H. Giessen, "Characteristics of supercontinuum generation in tapered fibers using femtosecond laser pulses," *Appl. Phys. B* **77**, 245–251 (2003).
36. T. A. Cerni, "An infrared hygrometer for atmospheric research and routine monitoring," *J. Atmos. Oceanic Tech-*

- no. **11**, 445–462 (1994).
37. M. F. Churbanov, I. V. Scripachev, G. E. Snopatin, V. S. Shiryayev, and V. G. Plotnichenko, “High-purity glasses based on arsenic chalcogenides,” *J. Optoelectron. adv. M.* **3**, 341–349 (2001).
38. W. Yuan, “2–10  $\mu\text{m}$  mid-infrared supercontinuum generation in  $\text{As}_2\text{Se}_3$  photonic crystal fiber,” *Laser Phys. Lett.* **10**, 095107 (2013).
39. B. Ung and M. Skorobogatiy, “Chalcogenide microporous fibers for linear and nonlinear applications in the mid-infrared,” *Opt. Express* **18**, 8647–8659 (2010).
- 

## 1. Introduction

Supercontinuum (SC) generation in the 2–5  $\mu\text{m}$  wavelength range of the mid-infrared (IR) attracts a lot of attention for applications in diverse fields including optical coherence tomography [1], biomedical technologies [2], and molecular spectroscopy [3]. The wavelength region between 2  $\mu\text{m}$  and 5  $\mu\text{m}$ , known as the molecular fingerprint region, is particularly important since a large number of molecules undergo strong vibrational transitions leaving unique absorption signatures. Demonstrations of mid-IR SC have been reported using fibers with different host materials such as chalcogenide (ChG) [4–8], bismuth [9, 10], fluoride [11, 12], and tellurite [13, 14]. However, there is a continued effort from researchers to develop all-fiber compact photonic devices that lower the power requirements for broadband mid-IR SC generation.

Mid-IR SC generation in ChG fibers such as  $\text{As}_2\text{Se}_3$  and  $\text{As}_2\text{S}_3$  is of a special interest due to their wide transparency window [15] and their high nonlinear refractive index ( $n_2$ ) that is up to  $\sim 930$  times that of silica [16]. A broadband SC in ChG fibers can be generated by shifting the zero-dispersion wavelength (ZDW) close to the central wavelength of the pump source. As a result, several structures of ChG fibers have been designed including microwires (also called nanowires) [17], microstructured [18] and tapered microstructured [19] fibers. Such fiber structures control the waveguide dispersion and increase modal confinement and nonlinearity [20].

In recent years, several experimental and theoretical investigations on mid-IR SC generation were reported in ChG microstructured fibers [5, 6, 14, 21–24] and microwires [25, 26]. For example, Mouawad et al. [24] reported SC generation from 0.6  $\mu\text{m}$  to 4.1  $\mu\text{m}$  in  $\text{As}_2\text{S}_3$  microstructured fibers from 200 fs pulses at a wavelength of 2.5  $\mu\text{m}$ . Marandi et al. [25] experimentally demonstrated SC from 2.2  $\mu\text{m}$  to 5.0  $\mu\text{m}$  in an  $\text{As}_2\text{S}_3$  microwire pumped by sub-100 fs pulses at a wavelength of 3.1  $\mu\text{m}$ . Shabahang et al. [27] obtained SC from 0.85  $\mu\text{m}$  to 2.35  $\mu\text{m}$  in composite ChG microwires using 1 ps pulses at a wavelength of 1.55  $\mu\text{m}$ . For fibers based on  $\text{As}_2\text{Se}_3$  ( $\sim 4 \times n_2$  of  $\text{As}_2\text{S}_3$  fiber [28]), SC from 2.1  $\mu\text{m}$  to 3.2  $\mu\text{m}$  was experimentally demonstrated using microstructured fibers [5] pumped with 100 fs pulses at a wavelength of 2.5  $\mu\text{m}$ . Using such fiber structures of  $\text{As}_2\text{Se}_3$ , theoretical investigations have shown the possibility of extending the SC up to a wavelength of 12  $\mu\text{m}$  under long pump wavelength condition [29, 30].

In  $\text{As}_2\text{Se}_3$  microwires, a SC from 1.15  $\mu\text{m}$  to 1.70  $\mu\text{m}$  was first demonstrated by Yeom et al. [17] using 250 fs pulses with an energy of 2.2 pJ and a wavelength of 1.55  $\mu\text{m}$ . Recently, we have shown that the extent of SC spectral broadening is limited by two-photon absorption at this pump wavelength [31]. We experimentally demonstrated a SC that spans from 1.26  $\mu\text{m}$  to 2.20  $\mu\text{m}$  by using a 90 fs Raman soliton with an energy of 14 pJ and a wavelength of 1.77  $\mu\text{m}$ . However, a SC in the 2–5  $\mu\text{m}$  wavelength range has yet to be demonstrated using  $\text{As}_2\text{Se}_3$  microwires. To generate a SC covering most of the 2–5  $\mu\text{m}$  spectral band, the challenge remains to design a microwire with the proper dispersion profile and selecting the appropriate pumping conditions.

In this paper, we demonstrate the first use of  $\text{As}_2\text{Se}_3$  microwires to generate a SC in the mid-IR. To achieve a SC in this spectrum range, we use pump pulses of 800 fs duration at a wavelength of 1.94  $\mu\text{m}$ . The SC covers a bandwidth of two octaves from 1.1  $\mu\text{m}$  to 4.4  $\mu\text{m}$ , and this exceeds the broadest reported SC spectrum in  $\text{As}_2\text{Se}_3$  microwires by a factor of 3.5. The combination of the microwire geometry and the highly nonlinear  $\text{As}_2\text{Se}_3$  glass results in

the realization of mid-IR SC at low pump power levels. The use of relatively long pulses of 800 fs prevents significant changes of their temporal and spectral profile while propagating in the untapered and transition regions of a tapered fiber (see e.g. [32]).

## 2. Experimental setup

Figure 1 shows a schematic of the SC source. The pump laser is a Tm-doped mode-locked fiber laser emitting pulses centered at a wavelength  $\lambda = 1.94 \mu\text{m}$  with a FWHM duration of 800 fs, an energy up to 180 pJ, at a repetition rate of 30 MHz, and an average power of 5.4 mW. A Tm-doped amplifier is used to elevate the source pulse energy up to 2.6 nJ. Along the Tm-doped amplifier, the pulse experiences anomalous dispersion and temporally broadens to a FWHM duration of 3.0 ps. A variable optical attenuator is inserted to control the pulse energy delivered to the input of the microwire. A Fourier Transform Infrared Spectrometer (FT-IR) is used to measure the generated SC spectra from the  $\text{As}_2\text{Se}_3$  microwire. The detection range of the FT-IR is bounded by the spectral range from 1 to  $5 \mu\text{m}$ .

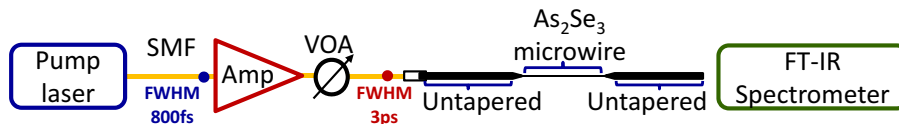


Fig. 1. Experimental setup for SC generation. SMF: single-mode fiber. VOA: Variable optical attenuator. Amp: Tm-doped amplifier.

## 3. $\text{As}_2\text{Se}_3$ microwire design

The  $\text{As}_2\text{Se}_3$  microwire is prepared from an  $\text{As}_2\text{Se}_3$  fiber that has a core/cladding diameter of  $6/170 \mu\text{m}$  and a numerical aperture of 0.2. The fiber is first pre-tapered to a core diameter of  $5.2 \mu\text{m}$  to match the mode-field distribution in a silica SMF. One of the end-face is polished and butt-coupled to a standard silica SMF. The Fresnel reflection, mode-mismatching, and the degree of alignment at the SMF- $\text{As}_2\text{Se}_3$  interface induce a measured coupling loss of  $\sim 1.6 \text{ dB}$ . Using the tapering process described in [33], a 1 cm long section in the central part of the fiber is heated and stretched into a 10 cm long microwire, resulting in a tapering loss of 2 dB. This is because of the surface scattering loss in the microwire region [34]. The fabricated tapered fiber thus consists of an untapered input section, a transition region, a microwire section, a transition region, and an untapered output section. The output end of the fiber is polished and left unconnected. The light emerging from the tapered fiber output travels through an open-air path before reaching the FT-IR.

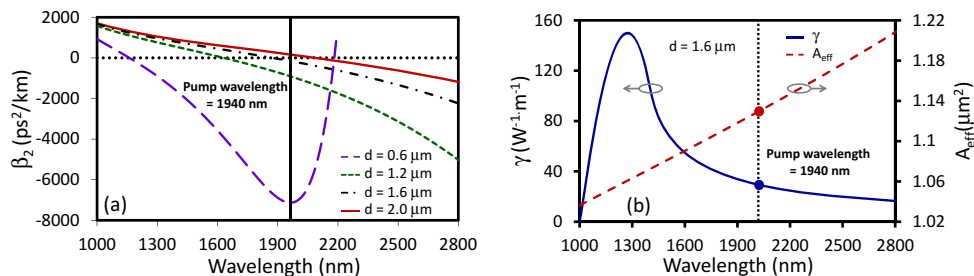


Fig. 2. a) Dispersion profiles of  $\text{As}_2\text{Se}_3$  microwire with diameters varying between  $0.6 \mu\text{m}$  and  $2.0 \mu\text{m}$ . b) Waveguide nonlinearity and effective mode area of  $\text{As}_2\text{Se}_3$  microwire with a diameter of  $1.6 \mu\text{m}$ .

Efficient SC generation in the microwire requires precise control of the group velocity dispersion (GVD) profile. Figure 2(a) shows the calculated GVD versus wavelength for several  $\text{As}_2\text{Se}_3$  microwire diameters, while Fig. 2(b) depicts the waveguide nonlinearity ( $\gamma$ ) and effective mode area ( $A_{\text{eff}}$ ) of  $\text{As}_2\text{Se}_3$  microwire with a diameter of  $1.6 \mu\text{m}$ . For the microwire with a diameter of  $1.6 \mu\text{m}$ , the pump pulse lies close to the ZDW ( $\sim 1.85 \mu\text{m}$ ) in the anomalous dispersion regime with  $\beta_2 = -130 \text{ ps}^2/\text{km}$ ,  $A_{\text{eff}} = 1.13 \mu\text{m}^2$  and  $\gamma = 32.2 \text{ W}^{-1}\text{m}^{-1}$ . This pump condition is ideal to achieve maximum spectral broadening [35].

#### 4. Results and discussion

##### 4.1. Mid-IR SC using pump laser without amplification

To obtain the optimal microwire diameter for maximum spectral broadening, the SC is measured experimentally using microwires of various diameters. For these measurements, the SC spectra are generated using the 800 fs pump laser at maximum output average power, and without the Tm fiber amplifier. Figure 3(a) shows the resulting spectra as a function of microwire diameters. The maximum spectral broadening is obtained from the microwire with a diameter of  $1.6 \mu\text{m}$ .

Next, the optimal microwire diameter for SC generation with a diameter of  $1.6 \mu\text{m}$  is pumped at various power levels. Figure 3(b) depicts the experimentally generated (solid-lines) SC spectra from the  $1.6 \mu\text{m}$  microwire diameter as a function of the pump pulse energy. The pulse energy values presented in the figure take into consideration the coupling loss to the tapered fiber and corresponds to a soliton number that increases from  $\sim 35$  to 87. At the pulse energy  $E_p = 124 \text{ pJ}$ , the spectrum covers a spectral bandwidth from  $1.43 \mu\text{m}$  to  $2.65 \mu\text{m}$  at 20 dB below the peak value.

To confirm the experimental results, numerical simulations of SC generation are also performed by solving the generalized nonlinear Schrödinger equation, using the Runge-Kutta interaction picture method. Due to shot-to-shot fluctuations in the input spectra, an ensemble of 20 simulations are carried with different initial random noise seeds for each input pulse. The mean spectrum of this ensemble is also averaged using a bandwidth resolution which is comparable to laboratory measurements to mimic the finite spectrometer spectral resolution.

Figure 3(b) shows also the numerically calculated SC spectra in dashed-lines as a function of

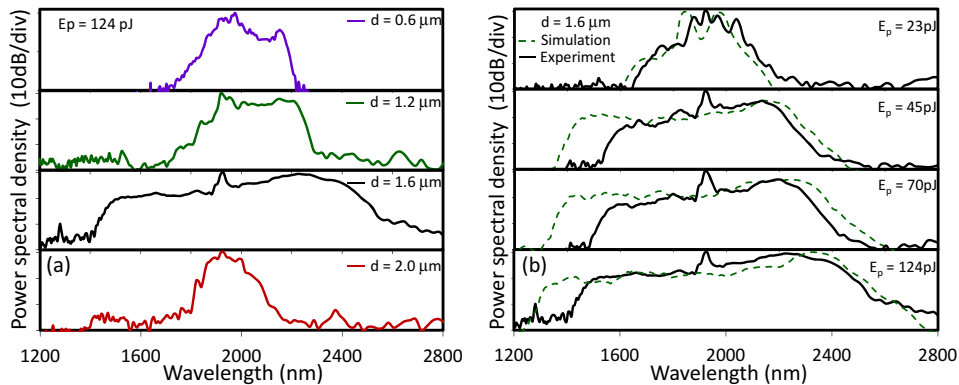


Fig. 3. a) Experimentally generated SC spectra from  $\text{As}_2\text{Se}_3$  microwires with diameters varying between  $0.6 \mu\text{m}$  and  $2.0 \mu\text{m}$ . The input pulse energy to the microwires is  $124 \text{ pJ}$ . b) Experimentally generated (solid-line) and calculated (dashed-line) SC spectra from a microwire with a diameter of  $1.6 \mu\text{m}$  using various pump power levels.

the pump pulse energy. The numerical simulations and the experimentally measured SC spectra agree reasonably well. In the numerical simulation, an 800 fs sech pulse profile is assumed to propagate a path of 370 cm along a SMF, through a 3 cm untapered input section length, 4.4 cm transition regions (both sides of the microwire), a 10 cm microwire, and a 1 cm untapered output section. The pulse is discretized into  $2^{14}$  samples with a temporal window width of 64 ps. The higher-order dispersion terms are included up to 9th order. The contribution of self steepening and the delayed Raman response are included with  $f_R = 0.1$ ,  $\tau_1 = 23$  fs and  $\tau_2 = 195$  fs are chosen to best fit with the experimental measurements [6] of the Raman gain spectrum in  $As_2Se_3$ . Two-photon absorption  $TPA(\lambda)$  [31],  $\alpha(\lambda)$  (i.e. intrinsic, coupling, and fabrication losses), Kerr nonlinearity index  $n_2(\lambda)$ , and effective mode area  $A_{eff}(\lambda)$  curves are also used for the simulation.

#### 4.2. Mid-IR SC using amplified pump laser

To extend the SC broadening further to the mid-IR, the pump laser is amplified using the Tm fiber amplifier. The bottom plot in Fig. 4 depicts the pump pulse spectrum before and after amplification together with the measured autocorrelation trace of the amplified pulse. Observation of the superimposed spectra reveals that the amplifier has no influence on the increase in pump pulse spectral width. However, the measured autocorrelation trace indicates that the amplifier contributes to temporal-profile broadening from chromatic dispersion, bringing the amplified pulsewidth to a duration of 3.0 ps. This pulsewidth value corresponds to autocorrelation duration of 4.2 ps. After amplification, the pulse energy reaches 2.5 nJ. The pulse is then sent to an attenuator to control its energy at the entrance of the tapered fiber. In the untapered input section and transition region of the tapered fiber, the amplified pulse experiences normal dispersion and compensates most of its temporal broadening without undergoing significant spectral broadening. SC generation occurs in the microwire section of the tapered fiber. Figure 4 also depicts

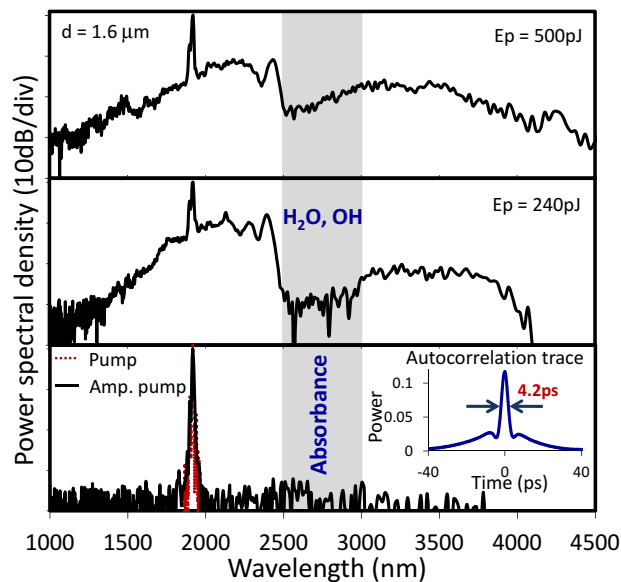


Fig. 4. Experimentally generated SC spectra from amplified pump pulses using a microwire with a diameter of  $1.6 \mu\text{m}$  and for various amplified pump power levels. The inset in the bottom plot shows the autocorrelation trace of the amplified pump pulse.

the experimentally generated SC spectra from amplified pulses of  $E_p = 240$  pJ and  $E_p = 500$  pJ using a  $1.6 \mu\text{m}$  microwire diameter of 10 cm long. The broadest spectrum extends from  $1.10 \mu\text{m}$  to  $4.40 \mu\text{m}$  at -30 dB and from  $1.46 \mu\text{m}$  to  $3.70 \mu\text{m}$  at -20 dB relative to the peak value. The dip in the spectra beyond  $2.50 \mu\text{m}$  is attributed to the water vapor absorption in the surrounding air [36] while traversing the 1.25 m path length inside the FT-IR and between the fiber and the FT-IR. The dip is also linked to the OH impurity band in  $\text{As}_2\text{Se}_3$  which is centered around a wavelength of  $2.90 \mu\text{m}$  [37]. This leads to a reduction in the energy carried at wavelengths beyond the OH impurity absorption band. The ratio of energy transfer to the mid-IR regime can be enhanced by using pump sources of higher pulse energy [29], sources operating at longer wavelengths [30, 38, 39], or by purifying the  $\text{As}_2\text{Se}_3$  glass from impurities [37].

## 5. Conclusion

In conclusion, we have demonstrated SC generation in the mid-IR regime using an  $\text{As}_2\text{Se}_3$  microwire of 10 cm long and a diameter of  $1.6 \mu\text{m}$ . The SC is generated by pumping with low energy pulses of only 500 pJ at a wavelength of  $1.94 \mu\text{m}$ . The generated spectrum covers a broad spectral bandwidth region spanning from  $1.1 \mu\text{m}$  to  $4.4 \mu\text{m}$ . The realization of the  $3.3 \mu\text{m}$  bandwidth using low energy pulses is achieved by optimizing the microwire diameter and using the highly nonlinear  $\text{As}_2\text{Se}_3$  glass.

## Acknowledgments

The authors are thankful to the Team Grants program of the Fonds de Recherche Québécois pour la Nature et les Technologies